Available online at www.sciencedirect.com
ScienceDirect
Thin Solid Films 516 (2008) 1499–1502
www.elsevier.com/locate/tsf

Sol–gel cobalt oxide–silica nanocomposite thin films for gas sensing applications

V. Musat [a,*], E. Fortunato [b], A.M. Botelho do Rego [c], R. Monteiro [b]

[a] Department of Metals and Materials Science, "Dunarea de Jos" University of Galati, 800008 Galati, Romania
[b] Department of Materials Science, CENIMAT, Faculty of Sciences and Technology, New University of Lisbon, Campus da Caparica, 2829-516 Caparica, Portugal
[c] Department of Chemical and Biological Engineering, CQFM, Technical University of Lisbon, 1049-001 Lisbon, Portugal

Available online 9 August 2007

Abstract

Various metal oxide–silica nanocomposite films have been recently proposed as gas-sensitive materials. This paper presents results on cobalt oxide–SiO_2 mesoporous nanocomposite thin films templated by a cationic surfactant. The films were deposited on glass substrate by dip-coating process, using $[Co(CH_3COO)_2]\cdot 4H_2O$ and tetraethoxysilane (TEOS) as starting materials. The effect of withdrawal speed, number of layers and thermal treatment on the crystalline structure, morphology, Co-doping states, optical, electrical and gas sensing properties of the thin films has been investigated using X-ray diffraction, atomic force microscopy, X-ray photoelectron spectroscopy, optical transmittance and room temperature photoreduction–oxidation data.

Keywords: Mesoporous thin films; Cobalt oxide; Silica-based nanocomposites; Sol–gel; Gas sensor

1. Introduction

Various porous metal oxide–silica nanocomposite films with enhanced gas-sensitive properties have been proposed for gas sensors [1–9]. The porosity of matrix provides a path for the gas molecules to reach the functional oxide nanoparticles and the films show reversible change in resistance and/or optical transmittance in the VIS-NIR range when exposed to gases. CoO/SiO_2 nanocomposite films are particularly investigated for application as optical gas sensors materials for NO, CO and/or H_2 detection [1,8,9].

Surfactant templated mesoporous materials are amorphous or nanocrystalline inorganic frameworks with periodically arranged pores 2–50 nm in diameter [10]. According to IUPAC recommendations, three groups of micro-, meso- and macroporous structures are discriminated, based upon the effective width of the pores (channels), if the effective width of their channels is less than 2 nm, in the 2–50 nm range and larger than 50 nm, respectively [11]. Sol–gel is the most successful and attractive route to prepare low cost silica-based nanocomposite thin films [1–4,8,12]. The preparation of mesoporous (5–50 nm pores size) films using a cooperative organization of inorganic species and surfactants is a very promising technology for constructing novel advanced materials with specific functions based on their microstructure [13,14]. This paper presents the morphology, Co-doping chemical states, optical properties and photoreduction–oxidation behavior of cobalt oxide–SiO_2 mesoporous nanocomposite thin films templated by a cationic surfactant in a dip-coating sol–gel process.

2. Experimental

2.1. Films preparation

The sol used for films deposition was prepared by the addition of $[Co(CH_3COO)_2]\cdot 4H_2O$ ethanol solution and $CH_3(CH_2)_{15}N(CH_3)_3Br$ (CTAB) surfactant to the pre-hydrolyzed tetraethoxysilane (TEOS) solution. The equivalent molar ratio of SiO_2:CoO was 98:2 and the molar ratio of

* Corresponding author.
E-mail addresses: viorica.musat@ugal.ro, vio52musat@yahoo.com (V. Musat), elvira.fortunato@fct.unl.pt (E. Fortunato), pcd800@mail.ist.utl.pt (A.M. Botelho do Rego), rcm@mail.fct.unl.pt (R. Monteiro).

0040-6090/$ - see front matter © 2007 Elsevier B.V. All rights reserved.
doi:10.1016/j.tsf.2007.07.197

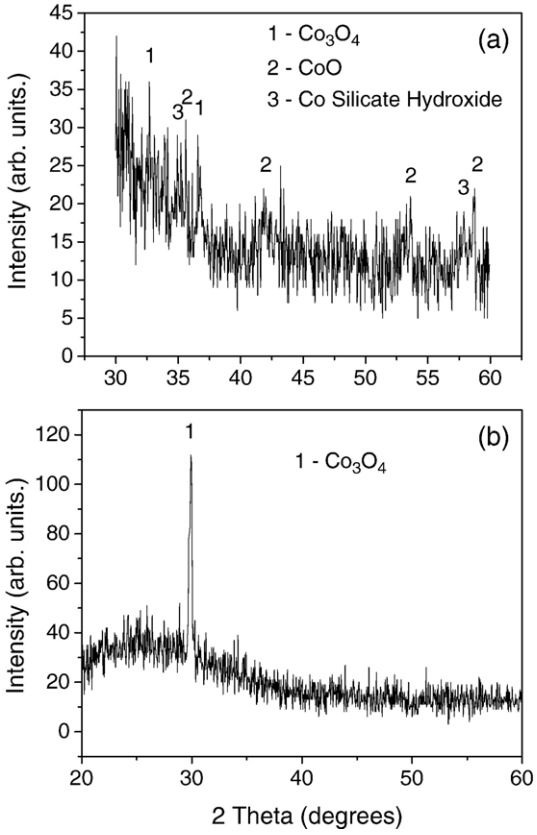

Fig. 1. XRD patterns of the films deposited at 30 cm/min, only pre-heat treated (a) and post-heat treated (b).

TEOS: C_2H_5OH:H_2O:HCl:CTAB was 1:25:7:0.14:0.05. The thin films (two layers) were deposited on soda lime glass substrate by dip-coating technique with different withdrawal speed values in the range 10–30 cm/min. After each layer deposition, the gel film was dried for 30 min at 70 °C and then pre-heated in air for 10 min at 400 °C. The procedure was repeated 2 or 3 times. The stabilized films were then post-heat treated 1 h in air at 500 °C for cobalt oxide crystallization. The thickness of the crystallized films (two layers), obtained from the ellipsometric data, had values of about 180 nm and about 290 nm when the withdrawal speed values of layer deposition were 10 cm/min and 30 cm/min, respectively.

2.2. Film characterization

The X-ray diffraction (XRD) patterns of the samples were recorded at room temperature using a Rigaku diffractometer (model RAD IIA), with CuKα radiation. The morphology on the surface and section of the films was analyzed using the atomic force microscopy (AFM). Tapping mode AFM experiments were performed in a Nanoscope IIIa Multimode AFM microscope (Digital Instruments, Veeco). Commercial etched silicon tips with typical resonance frequency of ca. 300 Hz (RTESP, Veeco) have been used as AFM probes. The chemical states (chemical environments) of the atomic species present in the films have been investigated by X-ray photoelectron spectroscopy (XPS), using a Physical Electronics 5600 Photoemission System and ultrahigh vacuum. The electrical resistivity of the films was measured in the dark, using a KEITHLEY 617 Model Programmable Electrometer. The optical transmittance was measured using a UV–VIS-NIR double beam spectrophotometer (Shimadzu, UV-3100 PC) in the wavelength range 200 to 2500 nm.

2.3. Sensing test

The gas (ozone) sensing properties were investigated by electrical measurements at room temperature, which were carried out *in* a special chamber presented elsewhere [15]. The conductivity of CoO film decreases when it is exposed in an ozone atmosphere. Because the films are in an insulating state, first, its conductivity is increased by photoreduction, when the films were directly irradiated in vacuum by the UV light of a mercury pencil lamp with an average intensity of 4 mW/cm^2, at 254 nm for 20 min. After that, the chamber was backfilled with oxygen at a pressure of 600 Torr and a UV lamp was used to produce ozone (the films are shielded from the lamp). The films were maintained for 40 min in this ozone atmosphere, when the re-oxidation of cobalt oxide crystallites results in a decrease of the film conductivity. An electric field of 50 V/cm was applied to the film sample and the electrical current was measured.

3. Results and discussions

Fig. 1 shows the XRD patterns of the films deposited at 30 cm/min, only pre-heat treated and post-heat treated. Generally, the only pre-heated films show a quasi amorphous microstructure with a very broad peak near $2\theta \approx 22°$ due to the SiO_2 aerogel matrix and local (short range) orderings corresponding to nuclei of CoO, Co_3O_4 and, most probably, cobalt silicate hydroxide crystalline phases (Fig. 1a) [16]. No very significant changes on XRD patterns take place when the films deposition withdrawal speed changes. The XRD pattern of the air post-heat treated film deposited at 30 cm/min (Fig. 1b) shows a sharp peak corresponding to a (220) orientated Co_3O_4 crystalline phase. AFM images on the surface of the thin films presented in Fig. 2 show cracks free malodorous films morphology with quasi-regularly shaped grains and regular roundish pores size depending on the withdrawal speed and thermal treatment. The surface roughness mean square (rms) of the pre-heated films, estimated from AFM measurements (2×2 μm surface), rises from 0.68 nm to 1.08 nm when the withdrawal speed increases from 10 cm/min to 30 cm/min, respectively. The post-heat treatment increases these rms values to 1.08 nm and 1.4 nm, respectively. The films deposited at 10 cm/min exhibit a more pronounced columnar structure (Fig. 2c). The surface topography image of the post-heated film (Fig. 2d) shows mesoporous morphology with regularly shaped columnar grains and regular roundish pores. Grain shrinkage but no densification takes place with film crystallization. A weak grains agglomeration tendency can be noticed.

XPS survey spectra of the only pre-heated films showed the presence of cobalt, silicon, oxygen and carbon. XPS data of the

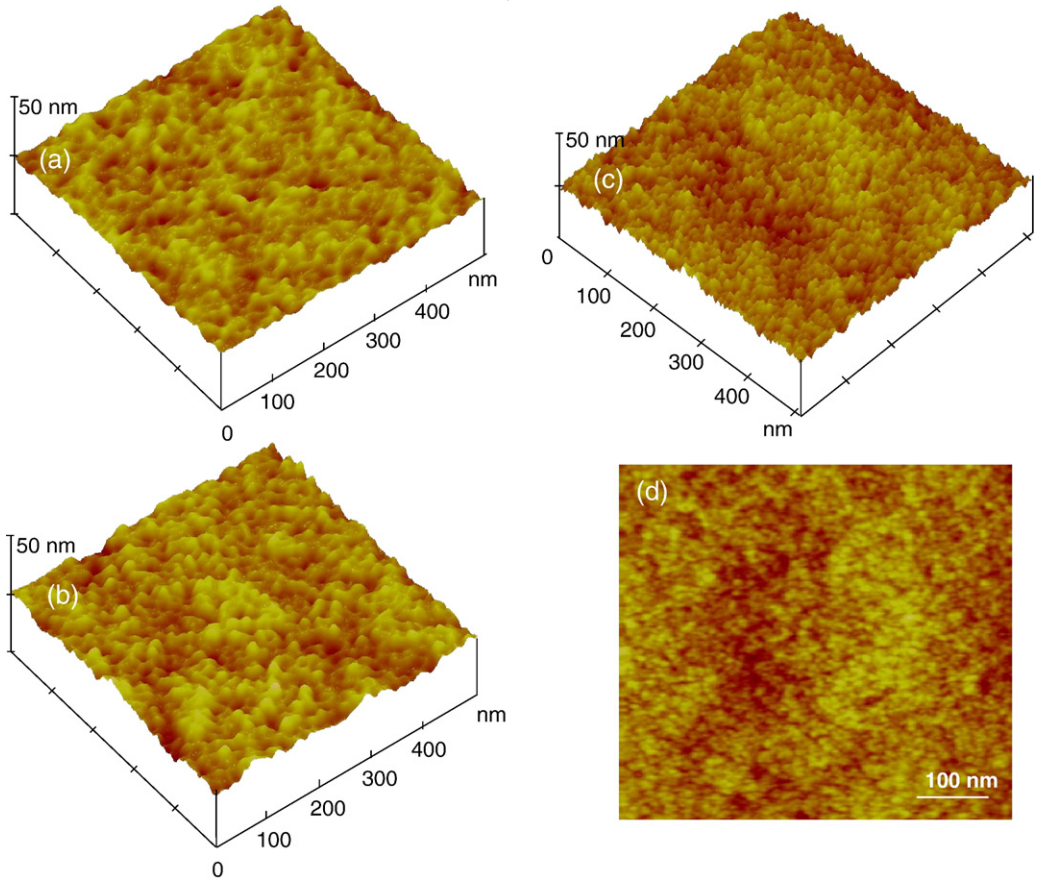

Fig. 2. AFM images of the pre-heated films deposited at 30 cm/min (a) and 10 cm/min (b) and of the post-heated films deposited at 10 cm/min (c, d).

non-cleaned surface films give cobalt surface composition 1% for all the samples. XPS spectra of Co $2p_{3/2}$ region of samples deposited at 10 cm/min and 30 cm/min showed three peaks (Fig. 3); two peaks at about 781.5 eV and 783.5–784 eV stemming from Co(II) oxide and Co(III) oxide, respectively, and a multiplet structure centered at 786.9–687.0 eV showing fine structure with several components caused by spin–spin interactions in the cobalt atoms (ions). The intensity of all these peaks increased when the withdrawal speed increased from 10 cm/min to 30 cm/min (Fig. 3). The relative importance of the components didn't change when withdrawal speed increased.

Electrical resistivity values between $6 \cdot 10^6$–$1 \cdot 10^7$ Ωcm have been measured in air for the post-heat treated films. Fig. 4 shows typical photoreduction–ozone oxidation cycles of the only pre-heated and the post-heat treated films deposited at 10 cm/min and of the post-heat treated films deposited at 30 cm/min. The conductivity of these thin films spontaneously increases by more than one order of magnitude after irradiation with UV light, while it rapidly decreases after exposure to oxidative ozone atmosphere. The photoreduction treatment by irradiation with UV light causes the formation of oxygen vacancies in the film, by transfer of oxygen from the bounds to the gaseous state. The remaining electrons increase the density of the free carriers, increasing the film conductivity. During the exposure of ozone, the oxygen vacancies are annihilated by re-oxidation and the film conductivity decreases again. The shape of the cycles showing the gas sensing response strongly depends on the thermal treatment of the films. Fig. 4a shows a slow response and a non-reversible photoreduction–reoxidation behavior of only pre-heat treated samples, whereas Fig. 4b

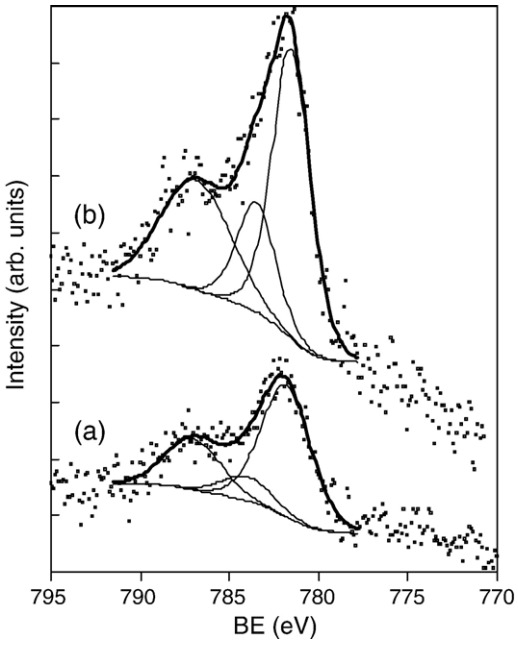

Fig. 3. XPS spectra of Co $2p_{3/2}$ region of the only pre-heat treated films deposited with 30 cm/min (a) and 10 cm/min (b).

and c show reversible sensing response of the post-heat treated films.

The optical transmittance of the films having 2 or 3 number of layers deposited with different withdrawal speed was higher than 85% within the visible and the near infrared region (Fig. 5). The detail in Fig. 5 shows the differences in the transmittance in the visible range (400–800 nm), depending on the withdrawal speed and the number of layers.

4. Conclusions

Very smooth and cracks free mesoporous cobalt oxide–SiO_2 nanocomposite films on soda lime glass substrate were prepared by dip-coating technique, using cetyltrimetylammonium bromide (CTAB) as surfactant, $[Co(CH_3COO)_2]\cdot 4H_2O$ and tetraethoxysilane (TEOS) as cobalt oxide and silica precursors, respectively.

Nuclei of CoO, Co_3O_4 and cobalt silicate hydroxide crystalline phases have been identified in the only pre-heat treated films (400 °C) and a (220) orientated Co_3O_4 crystalline phase was identified in the post-heat treated (500 °C) films. The presence of Co^{2+} and Co^{3+} states in the films has been confirmed from XPS data.

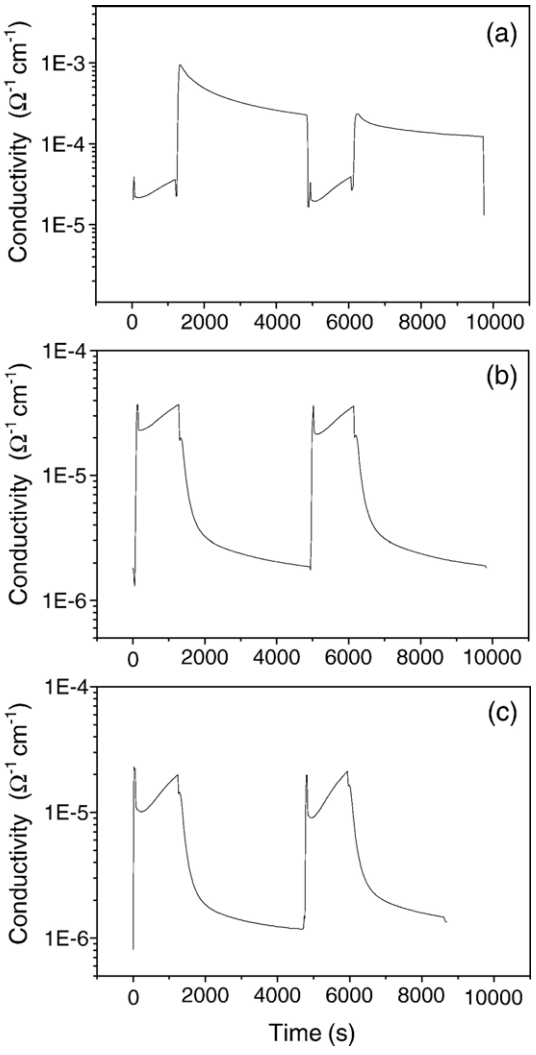

Fig. 4. Typical photoreduction–oxidation cycles (room temperature) of the only pre-heated films deposited at 10 cm/min (a) and of the post-heated films deposited at 10 cm/min (b), 30 cm/min (c).

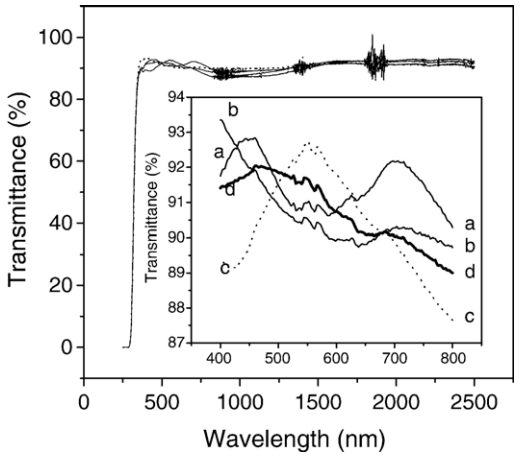

Fig. 5. Optical transmittance spectra of the post-heated films deposited with 30 cm/min 2 layers (a), 10 cm/min 2 layers (b), 10 cm/min 3 layers (c) and 3 cm/min, 2 layers (d).

The films show very good optical transmittance (between 85–95%) within the visible and near-IR wavelength region. The only pre-heat treated films show non-reversible photoreduction–reoxidation behavior, whereas the post-heat treated films show room temperature reversible gas sensing behavior.

Acknowledgments

This work was supported by NATO Expert Visiting PDD (CP)-CBP.EAP.EV 982079/2005 Grant.

References

[1] C. Cantalini, M. Post, D. Buso, M. Guglielmi, A. Martucci, Sens. Actuators, B, Chem. 108 (2005) 184.
[2] W.C. Chen, Mater. Lett. 59 (2005) 1239.
[3] S. Chakrabartini, D. Das, D. Ganguli, S. Chaudhuri, Thin Solid Films 441 (2003) 228.
[4] Y. Lu, L. Han, C.J. Brinker, T.M. Niemczyk, G.P. Lopez, Sens. Actuators, B, Chem. 35 (1996) 517.
[5] N. Carmona, M.A. Villegas, J.M. Fernández Navarro, Sens. Actuators, A, Phys. 116 (2004) 398.
[6] S. Shukla, S. Patil, S.C. Kuiry, Z. Rahman, T. Du, L. Ludwig, C. Parish, S. Seal, Sens. Actuators, B, Chem. 96 (2003) 343.
[7] T.C. Wang, C.L. Wu, Thin Solid Films 496 (2006) 658.
[8] L. Armelao, D. Barreca, S. Gross, A. Martucci, M. Tieto, E. Tondello, J. Non-Cryst. Solids 293 (2001) 477.
[9] N. Koshizaki, K. Yasumoto, T. Sasaki, Nanostruct. Mater. 12 (1999) 971.
[10] Z. Qi, I. Honma, H. Zhou, Anal. Chem. 78 (2006) 1034.
[11] L.B. McCusker, F. Liebau, G. Engelhardt, Microporous Mesoporous Mater. 58 (2003) 3.
[12] M. Ogawa, Chem. Commun. (1996) 1149.
[13] Y. Lu, R. Ganguli, C.A. Drewien, M. Anderson, C.J. Brinker, W. Gong, Y. Guo, H. Soyez, B. Dunn, M. Huang, J. Zink, Nature 389 (1997) 364.
[14] P. Innocenzi, A. Martucci, M. Guglielmi, A. Bearzotti, E. Traversa, C. Pivin, J. Eur. Ceram. Soc. 21 (2001) 1985.
[15] A. Pimentel, E. Fortunato, A. Gonçalves, A. Marques, H. Águas, L. Pereira, I. Ferreira, R. Martins, Thin Solid Films 487 (2005) 212.
[16] P. Dutta, B.C. Dunn, E.M. Eyring, N. Shah, G.P. Huffman, A. Manivannan, M.S. Seehra, Chem. Mater. 17 (2005) 5183.